

Nidogen 1 and Nuclear Protein 1: novel targets of ETV5 transcription factor involved in endometrial cancer invasion

Núria Pedrola¹ · Laura Devis¹ · Marta Llauredó¹ · Irene Campoy¹ · Elena Martínez-García¹ · Marta García¹ · Laura Muínelo-Romay² · Lorena Alonso-Alconada² · Miguel Abal² · Francesc Alameda³ · Gemma Mancebo⁴ · Ramon Carreras⁴ · Josep Castellví⁵ · Sílvia Cabrera⁶ · Antonio Gil-Moreno⁶ · Xavier Matias-Guiu⁷ · Juan L. Iovanna⁸ · Eva Colas^{1,7} · Jaume Reventós^{1,9} · Anna Ruiz^{1,10}

Received: 18 January 2015 / Accepted: 20 April 2015 / Published online: 30 April 2015
© Springer Science+Business Media Dordrecht 2015

Abstract Endometrial cancer is the most frequent malignancy of the female genital tract in western countries. Our group has previously characterized the upregulation of the transcription factor ETV5 in endometrial cancer with a specific and significant increase in those tumor stages associated with myometrial invasion. We have shown that ETV5 overexpression in Hec1A endometrial cancer cells induces epithelial to mesenchymal transition resulting in the acquisition of migratory and invasive capabilities. In the present work, we have identified Nidogen 1 (NID1) and Nuclear Protein 1 (NUPR1) as direct transcriptional targets of ETV5 in endometrial cancer cells. Inhibition of NID1 and NUPR1 in ETV5 overexpressing cells reduced cell migration and invasion in vitro and reduced tumor growth and dissemination in an orthotopic endometrial cancer model. Importantly, we

confirmed a significant increase of NUPR1 and NID1 protein expression in the invasion front of the tumor compared to their paired superficial zone, concomitant to ETV5 overexpression. Altogether, we conclude that NID1 and NUPR1 are novel targets of ETV5 and are actively cooperating with ETV5 at the invasion front of the tumor in the acquisition of an invasive phenotype to jointly drive endometrial cancer invasion.

Keywords ETV5 · NID1 · NUPR1 · Invasion · Endometrial cancer

Abbreviations

EMT	Epithelial to Mesenchymal Transition
NID1	Nidogen 1
NUPR1	Nuclear Protein 1
H	Hec1A cells
HG	Hec1A cells transfected with the pEGFP-C2 vector alone
HGE	Hec1A cells transfected with the pEGFP-hETV5

Jaume Reventós and Anna Ruiz have contributed equally to this work.

Electronic supplementary material The online version of this article (doi:10.1007/s10585-015-9720-7) contains supplementary material, which is available to authorized users.

✉ Eva Colas
ecolas@irbllleida.cat

✉ Anna Ruiz
annaruizn@gmail.com

¹ Biomedical Research Group in Gynaecology, Hospital Universitari Vall d'Hebron, Institut de Recerca (VHIR), Universitat Autònoma de Barcelona, Passeig Vall d'Hebron, 119-129, 08035 Barcelona, Spain

² Translational Laboratory/Medical Oncology Department, Complejo Hospitalario Universitario de Santiago/SERGAS, Santiago De Compostela, Spain

³ Pathology Department, Hospital del Mar, Barcelona, Spain

⁴ Gynecology Department, Hospital del Mar, Barcelona, Spain

⁵ Pathology Department, Vall d'Hebron University Hospital, Barcelona, Spain

⁶ Gynecological Oncology Department, Vall d'Hebron University Hospital, Barcelona, Spain

⁷ Pathology Department, Hospital Arnau de Vilanova, Lleida, Spain

⁸ INSERM U1068, CRCM, Cell Stress, Marseille, France

⁹ Basic Sciences Department, Universitat Internacional de Catalunya, Barcelona, Spain

¹⁰ Genetics Department, UDIAT, Corporació Sanitària Parc Taulí Institut Univesitari (UAB), Barcelona, Spain

HGEshNID1	HGE with downregulation of NID1
HGEshNUPR1	HE with downregulation of NUPR1
HGEshC	HE with shControl
ChIP	Chromatin immunoprecipitation
RTqPCR	Real time quantitative PCR

Introduction

Endometrioid endometrial cancer has a favorable prognostic due to an early diagnosis related with the early appearance of symptoms [1]. However, 20 % of patients present myometrial infiltration and/or lymph node affection at diagnosis. As the initial event in tumor invasion, myometrial invasion is one of the most valuable prognostic factors and determines an increase in the rate of recurrence after the first surgical treatment and a decrease in the 5 year survival follow-up [2]. Thus, unraveling the initial steps associated with myometrial infiltration may represent an important improvement in the identification of new therapeutic targets that prevent cancer dissemination.

The molecular pathology of myometrial invasion correlates with the down regulation of E-cadherin and the induction of an Epithelial to Mesenchymal Transition (EMT) [3, 4]. EMT is a crucial process in tumor invasion where cells lose their epithelial polarity and cell-to-cell contacts and acquire mesenchymal properties. EMT involves the loss of intercellular cohesion and the modification of the cytoskeleton, leading to increased motility and invasion. Transformed cells can detach, penetrate through the basement membrane and infiltrate surrounding tissues [5, 6].

Our group has previously characterized the upregulation of the transcription factor ETV5 in endometrial cancer with a specific and significant increase in those tumor stages associated with myometrial invasion [7, 8]. We have shown that ETV5 overexpression in an endometrial cancer cell line promotes cell migration and invasion through the activation of the matrix metalloprotease MMP2 [9]. In addition, we have demonstrated a role of ETV5 on the induction of EMT through the upregulation of ZEB1 expression and E-cadherin repression resulting in the acquisition of migratory and invasive capabilities [10]. To further characterize the initial steps of myometrial invasion regulated by the ETV5 transcription factor, we analyzed by gene expression microarray technology those genes whose expression was altered in Hec1A endometrial cancer cells with stable overexpression of a fusion GFP-ETV5 protein [10].

In the present work, we have identified Nidogen1 (NID1) and Nuclear Protein 1 (NUPR1) as direct transcriptional targets of ETV5. Both genes mediate some of the migratory and invasive capabilities induced by ETV5 overexpression in endometrial cancer cells both in vitro

and in vivo. Importantly, NID1 and NUPR1 were upregulated at protein and mRNA level at the invasive front of endometrial cancer tissues, concomitant with ETV5 overexpression.

Materials and methods

Cell lines and tumor samples

The human endometrial cancer cell line, Hec1A, was cultured as previously described by Monge et al. [9]. Tissue specimens were collected from patients who underwent surgery for endometrial cancer in the Departments of Gynaecological Oncology at the Hospital Vall d'Hebron and the Hospital del Mar in Barcelona (Barcelona, Spain). The Institutional Review Boards approved the protocol to perform this study and informed consent was obtained from all patients included. None of the patients had received radiation, hormonal therapy or chemotherapy prior to surgery. A total of 32 endometrial cancer samples were used to analyze the mRNA expression of NID1, NUPR1 and ETV5, and 9 paired samples of superficial and deep tumor were used to analyze the mRNA expression of NID1 and NUPR1 (Supplementary Table 1). We used a total of 82 paraffin-embedded tissues from endometrial cancer and controls (Supplementary Table 2), and paired superficial and deep sections of 116 paraffin-embedded tissues (Supplementary Table 3) to analyze the protein expression of ETV5, NID1 and NUPR1. Clinico-pathological data of each tumor is detailed in the indicated supplementary tables. Histological grading is based with regard to the degree of differentiation of the adenocarcinoma [11]. FIGO stage classification is based in the revised version published in 2009 [12].

Constructs and stable cell line generation

Hec1A cells either transfected with the pEGFP-C2 vector alone (HG) or the pEGFP-hETV5 (HGE) were selected with G-418 as described [9]. To generate stable cell lines with downregulation of NID1 (HGEshNID1) and NUPR1 (HGEshNUPR1) and control cells (HGEshC), we used lentiviral vectors carrying a CMV-driven Lac Z gene packaged with attenuated HIV-derived constructs and pseudotyped with VSV-G envelope, prepared by transient transfection of 293T cells, together with pGIPZ against NID1, NUPR1 or control (ABgene, Thermo Fisher Scientific). The following short hairpins against NID1 and NUPR1 were selected to generate stable HGE modified cell lines: shNID1a, 5'-ATCATAGCAGGTTTCGCCCG-3', and shNUPR1b, 5'-TCTCTCTTGGTGCGACCTT-3'. The transfection was carried out using Lipofectamine 2000

Table 1 Differentially expressed genes between ETV5 overexpressing cells and control cell line

Gene	FC	<i>P</i> value	Forward	Reverse	5 % DMSO	Annealing Temp
ANGPT-2	3.18	8.77E–15	5'-GAAGTCCTGACCTATTTGTAG-3'	5'-TCTCCCCAGATCCTACAGTG-3'	No	58 °C
PLOD2a	3.16	8.64E–17	5'GAAAGAGTCTAAGGCTCTCTTG-3'	5'-CACTTAGCTTTGGGAGTGGGTT-3'	Yes	56 °C
PLOD2b	3.16	8.64E–17	5'-AACCCACTCCCAAAGCTAAGTG-3'	5'-GCAGCTGAGGCTTACCCTGC-3'	Yes	56 °C
NUPR1a	2.8	3.31E–14	5'-CATTTGATCCTCTCCCAAC-3'	5'-GATTATAGACATCTGCCACC-3'	No	54 °C
NUPR1b	2.8	3.31E–14	5'-AAGTGTGCTGATATCCCTTC-3'	5'-CTTCTCCTAACGCTTTGTCT-3'	No	51 °C
EFNA5a	2.33	9.33E–10	5'-GAGTTGGAGGGATCCATTTG-3'	5'-GATAGAGGGCTTCGCGCTTG3'	No	50 °C
EFNA5b	2.33	9.33E–10	5'-ACACAGCTTGGCACCTCTTC-3'	5'-CATCTCCACGTGCAACATCAC3'	No	52 °C
NPR3a	1.78	1.09E–12	5'-ATTCCAGCGCAAACCTGCGTG-3'	5'-GGAGTCTCTCATTAACATTCT3'	Yes	58 °C
NPR3b	1.78	1.09E–12	5'-CGCTGCCACGCTATTTAAAC-3'	5'-CAAGAAAGAGCTTGCCCTC3'	No	60 °C
NID1a	1.8	1.74E–11	5'-GTTTCTTCTCCTCTTCAATGC-3'	5'-CCAAGTCATCAAAGACATTAG-3'	Yes	60 °C
NID1b	1.8	1.74E–11	5'-TTTCCACGTCGCCGGCTCTC-3'	5'-CATGTTCCCGAACTGCGGTC-3'	Yes	60 °C
LAMP3a	1.32	2.89E–09	5'-CAGCTGAAGAATCCAAGGCTC-3'	5'-TTTTCTAACAGCTCGGGTACC3'	No	62 °C
LAMP3b	1.32	2.89E–09	5'-CAGCCTGGCCAATATGGTGAC-3'	5'-GTTCTGCAGCGTGC GGCGAAG3'	Yes	62 °C

Fold change (FC) and *P* value of genes differentially expressed in the microarray analysis of HGE versus Hec1a cell lines [10]. For each gene, primers and PCR conditions used for ChIP analysis of their promoter regions. Letters behind the gene name (“a” or “b”) indicate different promoter regions for the same gene

(Invitrogen, Life technologies, Carlsbad, CA), following manufacturer’s instructions. Lentiviral supernatants were harvested 48 h after transfection and were filtered through 0.45 µm. Cleaned lentiviral medium was used to infect cells in the presence of 8 µg/mL polybrene. Transfected cells were selected with Puromycin (InvivoGen, San Diego, Ca, USA) at 1 µL/mL.

Chromatin immunoprecipitation assay

Chromatin immunoprecipitation (ChIP) on HGE cells was performed using rAb ERM/ETV5 and the Magna ChIP kit (Millipore, Billerica, MA), according to the manufacturer’s instructions and as previously described in Llauro et al. [13]. Melting temperatures and specific PCR conditions are described in Table 1.

Luciferase reporter assay

The human NID1 and NUPR1 promoters (promoter region comprising nucleotides from –375 to +3 and from –444 to –30 from Transcription Starting Site, respectively) were cloned in pGL4.15 luciferase vector (pGL4.15-NID1 and pGL4.15-NUPR1) (Promega, Madison, WI, USA). H, HG and HGE cells were split into 24-well plates before transfection and were transfected with a mixture of 370 ng reporter luciferase vector, 30 ng renilla luciferase vector and Lipofectamine 2000 for 5 h with serum-free medium. After 36 h, cells were lysed and luciferase activity was determined using the Dual Luciferase Assay Kit (Promega, Madison, WI, USA). Data are presented as relative fold

activation between cells transfected with either pGL4.15-NID1 or pGL4.15-NUPR1, and the pGL4.15 empty vector. Three independent replicates were performed per experiment. The assay was performed three times.

Real time quantitative PCR (RTqPCR)

RTqPCR was performed as described previously by Llauro et al. [14]. We used ETV5-Hs00231790_m1, NID1-Hs00159600_m1 and NUPR1-Hs00202610_m1 probes, for the analysis of endometrial tumor and control, and superficial and deep tumor samples. The GAPDH-Hs9999905_m1 probe was used for normalization. For the analysis of endometrial cancer cell lines, we used the 18 s ribosomal RNA C6_4308329 probe for normalization. All probes were TaqMan® Gene Expression Assays (Applied Biosystems, Foster City, CA, USA). Fold change expression values were calculated with the ddCT-method. Hec1A cells and four healthy endometrial samples were used respectively as controls when cell lines or human samples were analyzed.

Protein extraction

Whole cell extracts were prepared using RIPA Buffer and quantified by BioRad DCTM Protein Assay (BioRad Laboratories, Hercules, CA, USA). Nuclear and cytoplasmic protein was extracted using the NE-PER Nuclear and Cytoplasmic Extraction Reagents Kit (Cat No. 78835, Thermo Scientific, USA), following manufacturer’s instructions. For medium secreted protein extraction, adherent cells were cultured in a p100 dish with 6 mL of serum-

free medium during 48 h. The medium was collected and 1:1 volume of 20 % trichloroacetic acid (TCA) was added drop by drop with agitation. After 10 min incubation on ice, the sample was centrifuged at 10,000g for 20 min. Then, the pellet was resuspended in 6 mL of 10 % TCA and centrifuged at 10,000g during 20 min. Finally, the pellet was washed with 3 mL of diethyl ether and centrifuged for 10 min at 10,000g. The pellet was finally resuspended in RIPA Buffer.

Immunoblot

Immunoblot was performed as described by Llauro et al. [13]. Primary antibodies used in this study were anti-ETV5 (sc-22807, Santa Cruz Biotechnologies, Santa Cruz, CA, USA), anti-NID1 (anti-hNidogen1, MAB2570, R&D Systems, Minneapolis, MN USA), anti-Nupr1 [15] and anti α -tubulin (2125, Cell Signalling, Danvers, MA). NID1 immunoblot was performed on secreted proteins isolated from media.

Tissue microarray and immunohistochemistry

Two tissue microarrays were constructed at the Pathology Department of the Vall d'Hebron University Hospital and at the Pathology Department of the Hospital del Mar (Barcelona, Spain) to study protein expression and localization of NID1, NUPR1 and ETV5 in tumor versus control tissues, and in superficial versus invasive areas of the same tumor. Representative areas from the tissue specimens were carefully selected and marked on individual paraffin blocks. Two tissue cores of 1 mm in diameter were obtained from each paraffin block and were precisely arrayed in a new paraffin block. 5 μ m sections were obtained from all tissue microarray paraffin blocks. NID1 and ETV5 were detected by indirect immunoperoxidase assay with citrate buffer pH9 for antigen retrieval. Sections were incubated with primary antibodies for 2 h at room temperature using 1:25 and 1:100 dilutions, respectively. Next, sections were incubated with peroxidase conjugated goat anti-rabbit and anti-mouse immunoglobulin (EnVision Dual System, DAKO, Glostrup, Denmark). The monoclonal anti-Nupr1 was used at 1:200. Sections were incubated with the primary monoclonal antibody made in rat at 4 °C overnight. After rinsing in PBS, the specimens were treated with peroxidase-labelled anti-rat immunoglobulin for 30 min. Endogenous peroxidase activity was quenched with 3 % H₂O₂. Sections were washed, and reactions were developed with diaminobenzidine, followed by counterstaining with hematoxylin. Antibodies used for immunohistochemistry staining were the same as for immunoblot. Two experienced pathologist evaluated the staining of the tissue microarray and calculated a *histoscore* based on the

percentage of stained cells and the intensity of the staining (ranging from 1 –weakly positive- to 3 -strongly positive). Histoscores were calculated from the sum of (1 \times % cells staining weakly positive) + (2 \times % cells staining moderately positive) + (3 \times % cells staining strongly positive) to a maximum of 300.

Cell proliferation assay

For the determination of cell proliferation, 1 \times 10⁵ cells were plated in triplicate on p96 plates in complete or in serum free medium. After 48 h, 20 μ L of CellTiter 96[®] AQueous reagent (Promega, Madison, WI, USA) was added to the medium. After 90 min, the absorbance of the plate was measured at 490 nm. All experiments were done in triplicate. Proliferation assays were performed a minimum of three times.

Transwell migraton assay

A total of 2.5 \times 10⁵ H, HG, HGE, HGEshC, HGEshNID1 and HGEshNUPR1 cells were seeded on a 8 μ m pore size transwell (BD Bioscience, Franklin Lakes, NJ, USA) on serum free media in triplicate and incubated for 48 h. The cells were fixed by 4 % paraformaldehyd and after washing the non-migratory cells, cells were stained with 1 % violet cresyl. The stained membranes were cut and violet cresyl was dissolved with acid acetic 10 % dilution and measured by 590 nm absorbance. All experiments were done in triplicate. Migration assays were performed a minimum of three times.

Cell inverted invasion assay

Invasion assay was performed as previously described by Muinelo-Romay et al. [16]. Briefly, cells were seeded at 5 \times 10⁵ cells/mL directly onto the opposite face of the 8 mm size pore membrane transwell (Corning, Lowell, MA, USA) and incubated for 5 h before turning right-side-up. Diluted matrigel (BD Bioscience, Franklin Lakes, NJ, USA) was placed over the upper well. Inserts were placed in serum-free medium while 10 % FBS complemented medium was applied on top of the Matrigel. Living cells were stained with 4 mM of calcein-acetoxymethyl ester (Invitrogen) and visualized by confocal microscopy after 15 days. Images were scanned every 5 μ m intervals using a 10 \times objective. To quantify the rate of invasion, mRNA was extracted from cells invading into the matrigel and GAPDH mRNA levels were measured by using TaqMan[®] Gene Expression Assays (Applied Biosystems). All experiments were done in triplicate. Invasion assays were performed a minimum of three times.

Adhesion assay

A total of 5×10^4 cells were seeded into laminin- and collagen I-coated coverslips and allowed to adhere for 20 and 40 min, respectively. Adherent cells were fixed and stained with 1:1,000 dapi and 1:200 phalloidin. Fifteen fields per coverslips were manually quantified using the FSX100 microscope (Olympus). All experiments were done in triplicate. Measurements were made in at least three independent experiments. Quantification of 15 fields is plot in bar graphs showing media and standard deviation of three independent experiments (t-Student's test, $**P = 0.001$; $*P = 0.05$).

Orthotopic animal model

Six-week old female athymic nude mice (Charles River Laboratories, Inc, Wilmington, MA) were used in this model. All the procedures regarding experimentation and animal care were performed according to the guidelines of the Spanish Council for Animal Care. The Ethics Committee for Animal Experimentation of our institution approved the protocol of this study. A total of 45 mice were inoculated by transmyometrial injection of HGEshC, HGEshNID1 and HGEshNUPR1 cells ($n = 15$ per group) as described by Cabrera et al. [17]. Mice that developed peritoneal metastases without showing tumor growth in the uterus were discarded. Mice were sacrificed seven weeks after the injection. During necropsy, a macroscopic evaluation was performed as described [17]. The fluorescence emitted from the cells was detected by the IVIS-Spectrum, digitalized and electronically displayed as a pseudo color overlay onto a gray scale animal image. Regions of interest (ROIs) from displayed images were drawn automatically around the primary tumor fluorescent signals and quantified as calibrated Radiant Efficiency units. All tissues were formalin-fixed and processed for routine histological examination. Hematoxylin-Eosin (H&E) staining was performed using routine histological procedures. Histological examination was carried out by an experienced pathologist.

Statistical analysis

Statistical analyses were performed using the Statistical Package for Social Science (SPSS, IBM, USA) version 16.0. Kolmogorov–Smirnov test was used to evaluate normality of the data, and accordingly, parametric and non-parametric tests were performed for each comparison. Parametric Student t-tests were performed to compare ETV5, NID1 and NUPR1 mRNA expression and percentage of stained cells between invasive and non-invasive

tumors. A paired *T* test was used to compare the percentage of stained cells between the superficial and the invasive front of the tumor. A non-parametric paired test (Wilcoxon test) was used to compare dCT between the superficial and the invasive front of the tumor. Mann–Whitney U test was used to compare means in cell migration, invasion and proliferation assays. The Spearman's rho test was applied to analyze the correlation between ETV5, NUPR1 and NID1 expression in human tumor samples. Differences between the groups were considered significant if the *P* value was lower than 0.05.

Results

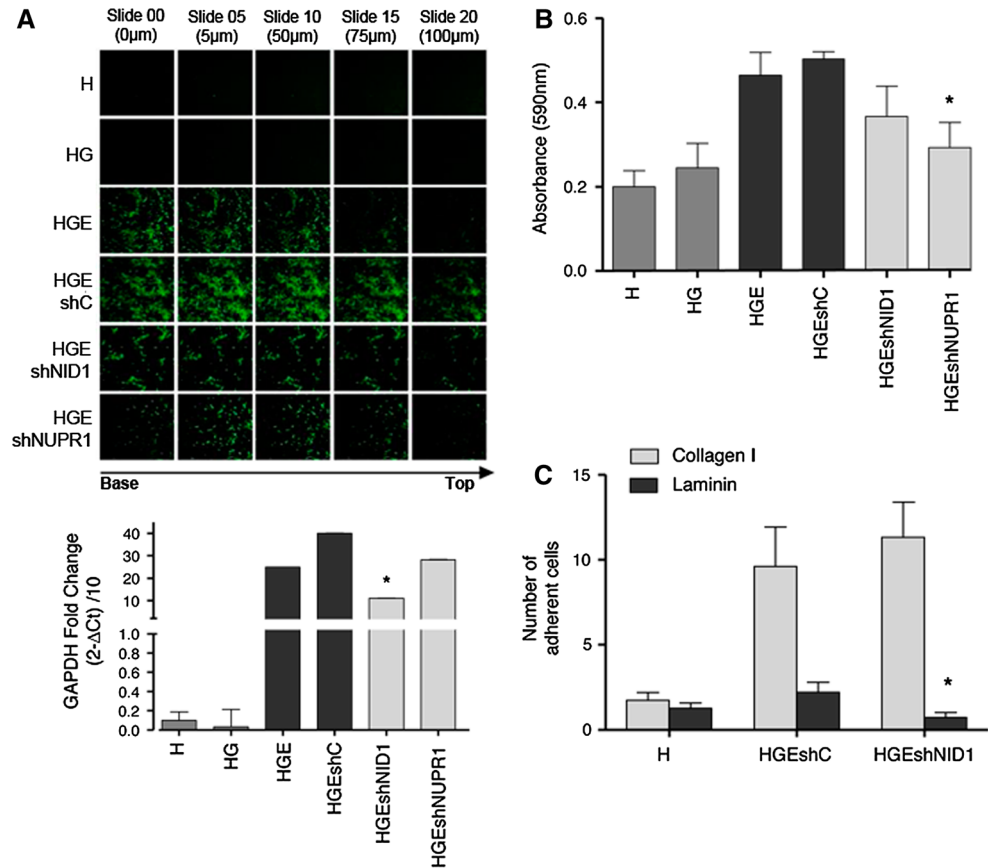
Identification of NID1 and NUPR1 as direct targets of ETV5 in Hec1A cells

In a previous work, gene expression profile of Hec1A endometrial cancer cells with overexpression of GFP-ETV5 (HGE) was compared to Hec1A control cells using microarray technology [10]. Based on the relative fold change ($FC > 1.3$) and putative ETS binding sites in their 5' putative promoter regions, seven selected genes (ANGPT-2, PLOD2, NUPR1, EFNA5, NPR3, NID1 and LAMP3) were analyzed by chromatin immunoprecipitation (ChIP) to determine whether ETV5 interacted with their 5' promoter regions (Table 1). ChIP analysis demonstrated that ETV5 did bind to the proximal promoter region of two of those genes, NID1 and NUPR1 (Fig. 1a). In order to further confirm ETV5 transcriptional regulation on NID1 and NUPR1, we analyzed whether ETV5 was able to induce the expression of a luciferase reporter gene under the control of NID1 or NUPR1 promoter regions. We found an increase in luciferase expression using both promoter regions when ETV5 was overexpressed, indicating that ETV5 directly regulates both genes at transcriptional level (Fig. 1b). Furthermore, ETV5 upregulation in Hec1A cell line was directly associated to an increased expression of NID1 and NUPR1 at mRNA level and NID1 at protein level (Fig. 1c, d). Upregulation of NID1 protein level was detected when analyzing the fraction of secreted proteins in the cell media but not in whole cell extracts. Altogether, we showed that ETV5 directly regulates NID1 and NUPR1 expression by binding to their 5' promoter regions.

Inhibition of NID1 and NUPR1 in HGE cells reduces cell migration and invasion in vitro

Previous work in our lab showed that ETV5 overexpression in Hec1A endometrial cancer cells induced an EMT phenotype and consequently, those cells improved their capabilities in cell scattering, migration and invasion both

Fig. 2 Inhibition of NID1 and NUPR1 in Hec1A endometrial cancer cells with GFP-ETV5 overexpression reduces cell migration and invasion in vitro. **a** *On top*, serial slides in a confocal microscopy of the inverted cell invasion assay. Optical sections were scanned at 5 μm intervals moving up from the underside of the membrane (*bottom*) into the Matrigel[®] (*top*). Calcein was used to stain cells in the matrigel. *On bottom*, RTqPCR of GAPDH mRNA levels of cells invading into Matrigel[®] were used to quantify the rate of invasion ($*P = 0.05$). **b** Quantification of fluorescent cells that migrate through a transwell well ($*P = 0.05$). **c** Hec1A cells, HGEsh control and HGEshNID1 were plated onto coverslips coated with collagen I and laminin to quantify cell adhesion. Quantification of 15 fields is plot in bar graphs showing media \pm sd of three independent experiments ($*P = 0.05$)



Altogether, these results confirmed that NID1 and NUPR1 are important downstream effectors to permit ETV5-dependent functions in a controlled in vitro model derived from Hec1A endometrial cancer cells. NID1 is associated to invasion of extracellular matrix with special affinity towards the laminin component, while NUPR1 is not involved in invasion but in the acquisition of migratory capabilities of HGE cells.

Tumor growth and dissemination are reduced upon inhibition of NID1 and NUPR1 in vivo

We used an endometrial orthotopic mouse model to analyze the effects of inhibiting NID1 and NUPR1 in HGE cells as this murine model represents a more realistic approach towards the process of dissemination of endometrial cancer. Thanks to this model, tumor cells are localized in the same microenvironment of the original tumor, so we could understand the process of tumor growth and myometrial infiltration under endometrial stimuli [17]. We inoculated 15 nude mice per experimental condition with one million HGEshC or HGEshNID1 or HGEshNUPR1 cells. Occurrence of endometrial tumor and metastasis occur in every group as we observed peritoneal implants, lymphatic dissemination and haematogenous metastasis in

the three groups of mice. In order to verify that inhibition of NID1 and NUPR1 were maintained through all the experiment, three representative sections of primary tumors and metastases were analyzed by immunohistochemistry against ETV5, NID1 and NUPR1 antibodies. As expected, we found expression of ETV5, NID1 and NUPR1 in HGEshC mice, whereas in HGEshNID1 and HGEshNUPR1 mice, ETV5 was expressed and NID1 and NUPR1 protein levels were reduced, respectively, compared to HGEshC (Supplementary Fig. 3a, b). Microscopically, all tumors showed an infiltrative phenotype, and necrotic areas probably as a consequence of tumor growth (Fig. 3c).

We quantified tumor size of primary tumors using the GFP fluorescence signal detected by the IVIS system, as all clones expressed GFP. Mice inoculated with HGEshNID1 cells developed smaller primary tumors than mice inoculated with HGEshC and HGEshNUPR1 (Fig. 3a). Interestingly, mice injected with HGEshNID1 and HGEshNUPR1 cells generated less metastases per mice compared to mice in the control group (Fig. 3b). Specifically, the number of haematogenous metastasis, corresponding to lung metastases, which are considered the most aggressive type of metastasis in patients, were lower in HGEshNID1 and HGEshNUPR1 mice than in control mice. Altogether, these results confirmed that in vivo, both

NID1 and NUPR1 maintain a role in distant dissemination associated to ETV5-dependent regulation and that NID1 could be also associated to tumor growth, probably related to its capability of remodeling the surrounding extracellular matrix.

Expression of NID1 and NUPR1 in human endometrial tumor samples

In order to evaluate the importance of these findings, it was crucial to translate our results in clinically relevant samples. To do that, we firstly verified whether an increase of ETV5 was associated with an increase in NID1 and NUPR1 during endometrial tumor invasion in human endometrial samples. We measured by RTqPCR the expression levels of NID1, NUPR1 and ETV5 in tumor endometrial samples corresponding to different FIGO stages. As expected, we observed significantly higher ETV5 mRNA expression levels in invasive tumors (FIGO stage IB and beyond, which are tumors that invade more than a half of the myometrium) compared with non-invasive tumors (FIGO stage IA) (Fig. 4a). We

found that NID1 mRNA levels were also higher in invasive tumors with a difference close to significant ($P = 0.071$). Interestingly, mRNA levels of both molecules were significantly correlated in our set of tumor samples (Fig. 4b). These results highlight the importance of both molecules in tumor progression and associate the expression of both molecules at the invasive front. By contrast, we could find neither a correlation between NUPR1 and ETV5 mRNA expression levels nor any association between NUPR1 mRNA levels and FIGO stage.

We further explore the role of NID1 and NUPR1 in tumor invasion by comparing the expression of these molecules in two areas of invasive tumors. Those two areas were macroscopically dissected by a pathologist and corresponded to a deep section of the tumor, which is the tumor in contact with the myometrial wall and where invasion takes place, and a superficial section. We only evaluated the expression of NUPR1 and NID1 genes as ETV5 has been described as specifically upregulated in the deep area of endometrial tumors in our previous work [10]. Now, we proved that NUPR1 is also increased in the deep

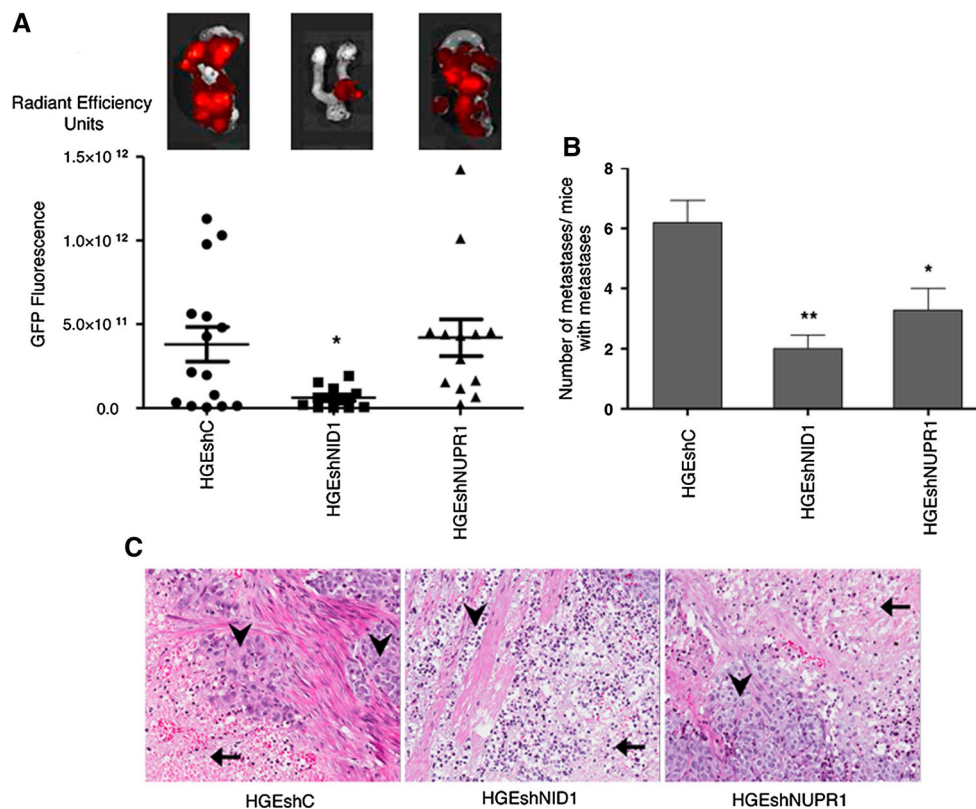


Fig. 3 Inhibition of NID1 and NUPR1 in HGE cells reduces tumor growth and dissemination in an orthotopic endometrial cancer model. **a** GFP fluorescence was used to quantify uterine primary tumour growth. GFP intensity was measured in radiant efficiency units within labelled ROIs (regions of interest) ($*P = 0.05$). *On top of each group*, a representative primary uterine tumor photographed by the IVIS system to detect the GFP fluorescence. **b** Number of metastasis found

in mice injected with HGEshC, HGEshNID1 and HGEshNUPR1 cells ($*P = 0.05$; $**P = 0.001$). **c** H&E staining of the orthotopically endometrial tumors showing the interface between the tumor and the myometrium (20 \times). The *head arrow* indicates the infiltrating tumor while the *black arrow* indicates necrosis as a consequence of tumor growth

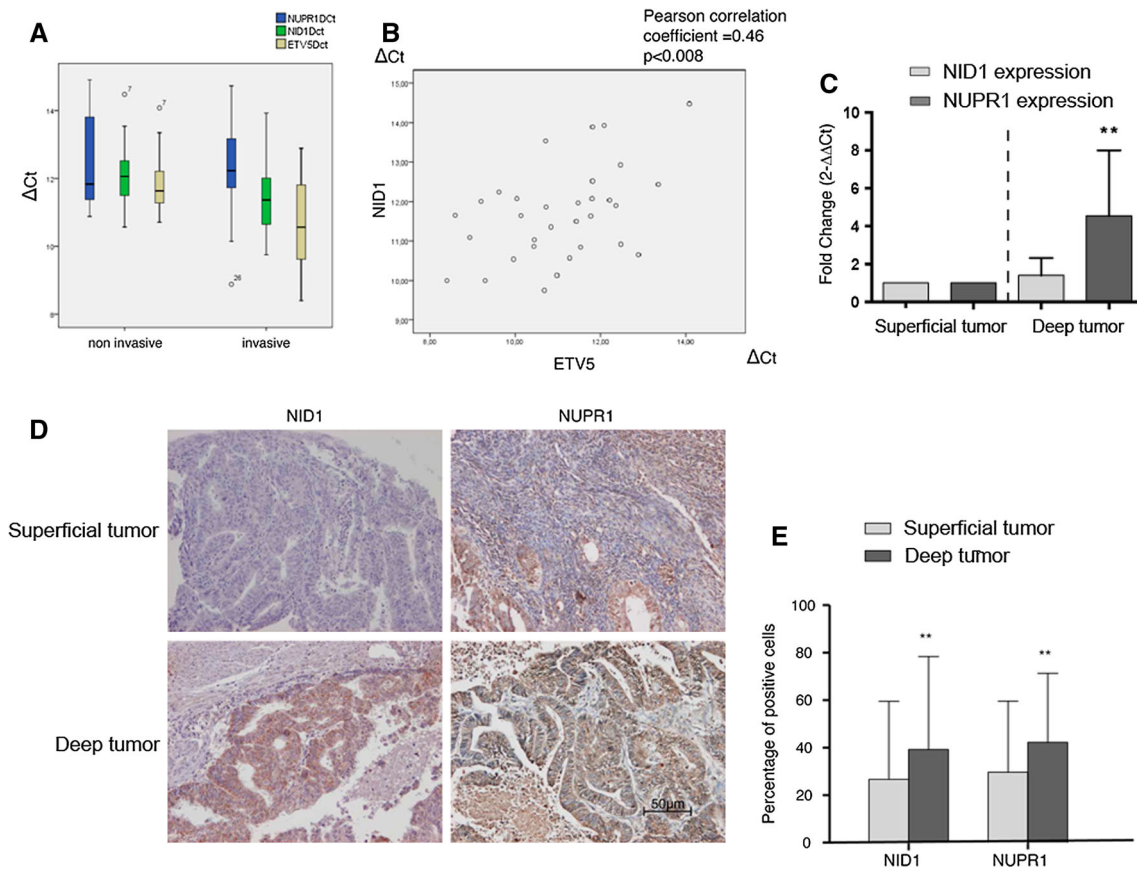


Fig. 4 NID1 and NUPR1 expression in human endometrial tumor samples. **a** NID1, NUPR1 and ETV5 mRNA expression levels are plotted as ΔC_T (target gene–endogenous gene) according to tumor invasiveness, measured as tumor stage IA (non invasive) versus tumor stage IB (invasive). GAPDH was used as endogenous gene. **b** Correlation between NID1 and ETV5 mRNA expressions in tumor samples (Pearson’s $r = 0.46$, $P = 0.008$). **c** RTqPCR analysis of

NID1 and NUPR1 in superficial and deep sections of tumors are plotted (** $P = 0.008$). **d** Immunohistochemistry of NID1 and NUPR1 in superficial and deep tumors. **e** Quantification of the percentage of NID1 and NUPR1 stained cells of a tissue microarray that includes the superficial and the invasive front of the tumor (** $P = 0.001$)

area of endometrial tumors, and hence, its expression is localized in the areas of invasion of endometrial cancer (Fig. 4c).

Finally, we studied NID1, NUPR1 and ETV5 expression at protein level in two human tissue microarray that included a total of 82 and 116 tissue specimens. Our analyses confirmed a significant correlation between ETV5 and NID1 in endometrial cancer samples (Pearson’s $r = 0.351$) and specifically, ETV5 showed correlation with NID1 and NUPR1 at the invasion front of endometrial tumors (Fig. 4d). Concomitant with ETV5 protein overexpression [10], we found a significant increase of NUPR1 and NID1 protein expression in the invasion front of the tumor compared to their paired superficial zone (Fig. 4e). To sum up, we proved that NID1 and NUPR1 are localized in areas where invasion takes place that are associated to ETV5 overexpression, and hence, we could speculate that NID1 and NUPR1 might be two key mediators of ETV5-dependent invasion in a realistic scenario.

Discussion

Endometrial cancer is the most frequent infiltrating tumor of the female genital tract, with myometrial invasion representing an increase in the rate of recurrences and a decrease in survival. Myometrial invasion represents the change in tumor FIGO classification from stage IA to stage IB, which is associated with tumor spread and relapse after primary treatment, resulting in a reduction in patient survival from 95 to 75 %.

Our group described the upregulation of ETV5 transcription factor in endometrial cancer associated to a phenotype that increase the ability of tumor cells to migrate and infiltrate the myometrium [8]. Specifically, we have been able to show that overexpression of ETV5 in Hec1A cells, which are derived from an endometrioid endometrial tumor stage IA, results in an Epithelial to Mesenchymal Transition [10]. In the present work we aimed to further characterize the molecular events involved in myometrial

invasion regulated by ETV5 transcription factor as we identify new molecules involved in cell migration and invasion in endometrial cancer.

We have found that ETV5 can bind to NID1 and NUPR1 promoter regions by ChIP assay and is able to induce the expression of a luciferase reporter under the control of NID1 or NUPR1 promoter regions, indicating that NID1 and NUPR1 are transcriptionally regulated by ETV5 in endometrial cancer cells through direct binding to its promoter regions. Its binding activates the expression of both genes at mRNA level, and NID1 at protein level. Importantly, we found that expressions of NID1 and ETV5 were correlated in human endometrial tumor samples at mRNA and at protein level, and specifically NID1 and NUPR1 were correlated with ETV5 at the deep tumor, where invasion takes place. Overexpression of three molecules was localized in the invasion front of the tumor at mRNA and protein level compared to their paired superficial zone. Altogether, we probed *in vitro* that NID1 and NUPR1 are directly regulated by ETV5, and we believe that this mechanism occurs in patients as both molecules are highly correlated with ETV5, especially at areas where tumor invasion occurs.

Tumor heterogeneity has been largely described. In particular, the invasive front is one of the areas of a tumor tissue where gene and protein expression has been observed to be dynamically adapted. Changes associated with the phenotype of the epithelial cells that become invasive have been described as well as tumor modifications induced by the microenvironment [19–22]. We suggest that NID1 and NUPR1 may mediate ETV5 induction of an invasive phenotype and in the modulation of the stroma to jointly drive cancer invasion.

NUPR1 (also called p8 and com-1) is a small protein related to the high mobility group of transcriptional regulators. It is involved in different biological functions such as endoplasmic-reticulum stress response, programmed cell death, cell cycle progression and the control of gene expression by regulating chromatin accessibility [23]. Knockdown of NUPR1 expression in ETV5 overexpressing cells (HGE) resulted in a decrease migration capability compared with control cells. Similar results have been reported by Sandi et al. who described that NUPR1 expression controls pancreatic cancer cell migration. Unlike Sandi et al. we could not find a decrease in cell invasion in HGE cells with downregulation of NUPR1 suggesting that in HGE cells invasion is mainly mediated by other ETV5 downstream molecules. [15]. Overexpression of NUPR1 in the invasion front may be related to other roles of NUPR1 in cell invasion such as tumor survival. NUPR1 has been shown to protect cells from stress-induced death by inhibiting apoptosis [24]. NUPR1 has been found to be overexpressed and to play a role in pancreatic,

pituitary, breast and thyroid cancer [25]. However, in prostate and bladder cancer NUPR1 appears to have tumor suppressive activity [26, 27]. In endometrial cancer, we showed that expression of NUPR1 is associated to the process of carcinogenesis as it is overexpressed at the invasive front of the tumors and is associated to migration *in vitro*.

NID1 is a glycoprotein located at the basement membrane that is secreted by mesenchymal cells and deposited at the cell surface and at cell junctions. Its major biological functions include extracellular matrix assembly, a role in homeostasis and wound healing, enhancement of cell attachment, chemotaxis and phagocytosis [18]. Overexpression of ETV5 results in the acquisition of a mesenchymal cell phenotype and increase in cell invasion. Knockdown of NID1 in ETV5 overexpressing cells showed a significant decrease in cell invasion. Cell invasion is a multistep process, which requires adhesion, proteolysis of extracellular matrix components and migration. We found a significant decrease in the adhesion to laminin and a moderate decrease in cell migration in cells with ETV5 overexpression and NID1 inhibition. The major role of NID1 is extracellular matrix assembly through its interaction with laminin and collagen IV [28, 29]. Recent studies have demonstrated that NID1 and other extracellular matrix proteins play important roles within the tumor microenvironment. Deposition of extracellular matrix proteins such as collagen I and IV, fibronectin, laminin and matricellular proteins leads to matrix remodelling and subsequent release of proteases such as metalloproteinases (MMPs) and cathepsins, which degrade the basement membrane and initiate a pro-invasion programme for tumour cells [30].

Finally, we showed in an orthotopic endometrial cancer model that tumors with NID1 inhibition were smaller than controls. In contrast, we did not observe an effect on the proliferation of cells with NID1 inhibition *in vitro* suggesting that secreted factors produced by the tumor cells and the microenvironment influence tumor growth *in vivo*. The average number of metastases was decreased when NID1 or NUPR1 were inhibited confirming our *in vitro* results. Similarly, it has been shown that mice injected with NUPR1 overexpression cells produced tumors whereas the mice injected with NUPR1-silenced fibroblasts did not [31]. Consistently, Sandi et al. described that xenograft pancreatic tumor development is dependent on NUPR1 expression [15].

In summary, our results show that ETV5 transcription factor regulates NID1 and NUPR1 transcriptionally and activates their expression. NID1 regulation by ETV5 enhances cell invasion and cell adhesion to the extracellular matrix, while NUPR1 regulation by ETV5 enhances cell migration in endometrial cancer. The increase in ETV5, NID1 and NUPR1 expression is preferentially at the invasion front of the tumor, where tumor cells infiltrate the

myometrium. To our knowledge this is the first study that describes a role of NID1 and NUPR1 in endometrial cancer carcinogenesis in vitro and in vivo. The data presented here contributes to the elucidation of the molecular mechanisms involved in endometrial cancer invasion. Limitations of this study included the lack of additional clinico-pathological parameters and follow-up of the patients, so further studies are needed to unveil the relation between NID1 and NUPR1 with other prognostic factors. The identification of NID1 and NUPR1 in endometrial tumor invasion may be useful to improve new therapeutic strategies in endometrial cancer aiming to increase the survival rate in endometrial cancer patients.

Acknowledgments We thank Marie-Noé Lavaut for technical assistance. This work has been supported by the Spanish Ministry of Science and Innovation (SAF2011-26548), the Spanish Ministry of Health (RD12/0036/0035), the AECC (Grupos Estables de Investigación 2011—AECC- GCB 110333 REVE), the Fundació La Marató TV3 (2/C/2013), the CIRIT Generalitat de Catalunya (2014 SGR 1330) and the European Commission EU FP7-PEOPLE-2010-IRSES (PROTBIOFLUID-269285). La Ligue Contre le Cancer, INCa, Cancerpole PACA, DGOS (labellisation SIRIC) and INSERM to JLI. EM is recipient of a fellowship from the Ministry of Education, Culture and Sport (Spain) (FPU12/05571).

References

- Amant F, Moerman P, Neven P et al (2005) Endometrial cancer. *Lancet* 366:491–505. doi:10.1016/S0140-6736(05)67063-8
- Siegel R, Naishadham D, Jemal A (2013) Cancer statistics, 2013. *CA Cancer J Clin* 63:11–30. doi:10.3322/caac.21166
- Colas E, Pedrola N, Devis L et al (2012) The EMT signaling pathways in endometrial carcinoma. *Clin Transl Oncol Off Publ Fed Span Oncol Soc Natl Cancer Inst Mex* 14:715–720. doi:10.1007/s12094-012-0866-3
- Tanaka Y, Terai Y, Kawaguchi H et al (2013) Prognostic impact of EMT (epithelial-mesenchymal-transition)-related protein expression in endometrial cancer. *Cancer Biol Ther* 14:13–19. doi:10.4161/cbt.22625
- Thiery JP (2002) Epithelial-mesenchymal transitions in tumour progression. *Nat Rev Cancer* 2:442–454. doi:10.1038/nrc822
- Yilmaz M, Christofori G (2009) EMT, the cytoskeleton, and cancer cell invasion. *Cancer Metastasis Rev* 28:15–33. doi:10.1007/s10555-008-9169-0
- Planagumà J, Gonzalez M, Doll A et al (2006) The up-regulation profiles of p21WAF1/CIP1 and RUNX1/AML1 correlate with myometrial infiltration in endometrioid endometrial carcinoma. *Hum Pathol* 37:1050–1057. doi:10.1016/j.humpath.2006.03.007
- Planagumà J, Abal M, Gil-Moreno A et al (2005) Up-regulation of ERM/ETV5 correlates with the degree of myometrial infiltration in endometrioid endometrial carcinoma. *J Pathol* 207:422–429. doi:10.1002/path.1853
- Monge M, Colas E, Doll A et al (2007) ERM/ETV5 up-regulation plays a role during myometrial infiltration through matrix metalloproteinase-2 activation in endometrial cancer. *Cancer Res* 67:6753–6759. doi:10.1158/0008-5472.CAN-06-4487
- Colas E, Muinelo-Romay L, Alonso-Alconada L et al (2012) ETV5 cooperates with LPP as a sensor of extracellular signals and promotes EMT in endometrial carcinomas. *Oncogene* 31:4778–4788. doi:10.1038/ncr.2011.632
- Creasman WT, Odicino F, Maisonneuve P et al (2006) Carcinoma of the corpus uteri. FIGO 26th annual report on the results of treatment in gynecological cancer. *Int J Gynaecol Obstet Off Organ Int Fed Gynaecol Obstet* 95(Suppl 1):S105–S143. doi:10.1016/S0020-7292(06)60031-3
- Creasman W (2009) Revised FIGO staging for carcinoma of the endometrium. *Int J Gynaecol Obstet Off Organ Int Fed Gynaecol Obstet* 105:109. doi:10.1016/j.ijgo.2009.02.010
- Llauradó M, Majem B, Castellví J et al (2012) Analysis of gene expression regulated by the ETV5 transcription factor in OV90 ovarian cancer cells identifies FOXM1 overexpression in ovarian cancer. *Mol Cancer Res MCR* 10:914–924. doi:10.1158/1541-7786.MCR-11-0449
- Llauradó M, Abal M, Castellví J et al (2012) ETV5 transcription factor is overexpressed in ovarian cancer and regulates cell adhesion in ovarian cancer cells. *Int J Cancer J Int Cancer* 130:1532–1543. doi:10.1002/ijc.26148
- Sandi MJ, Hamidi T, Malicet C et al (2011) p8 expression controls pancreatic cancer cell migration, invasion, adhesion, and tumorigenesis. *J Cell Physiol* 226:3442–3451. doi:10.1002/jcp.22702
- Muinelo-Romay L, Colas E, Barbazan J et al (2011) High-risk endometrial carcinoma profiling identifies TGF- β 1 as a key factor in the initiation of tumor invasion. *Mol Cancer Ther* 10:1357–1366. doi:10.1158/1535-7163.MCT-10-1019
- Cabrera S, Llauradó M, Castellví J et al (2012) Generation and characterization of orthotopic murine models for endometrial cancer. *Clin Exp Metastasis* 29:217–227. doi:10.1007/s10585-011-9444-2
- Chung AE, Dong LJ, Wu C, Durkin ME (1993) Biological functions of entactin. *Kidney Int* 43:13–19
- Kopfstein L, Christofori G (2006) Metastasis: cell-autonomous mechanisms versus contributions by the tumor microenvironment. *Cell Mol Life Sci CMLS* 63:449–468. doi:10.1007/s00018-005-5296-8
- De Wever O, Mareel M (2003) Role of tissue stroma in cancer cell invasion. *J Pathol* 200:429–447. doi:10.1002/path.1398
- Talbot LJ, Bhattacharya SD, Kuo PC (2012) Epithelial-mesenchymal transition, the tumor microenvironment, and metastatic behavior of epithelial malignancies. *Int J Biochem Mol Biol* 3:117–136
- Friedl P, Alexander S (2011) Cancer invasion and the microenvironment: plasticity and reciprocity. *Cell* 147:992–1009. doi:10.1016/j.cell.2011.11.016
- Brannon KM, Million Passe CM, White CR et al (2007) Expression of the high mobility group A family member p8 is essential to maintaining tumorigenic potential by promoting cell cycle dysregulation in LbetaT2 cells. *Cancer Lett* 254:146–155. doi:10.1016/j.canlet.2007.03.011
- Hamidi T, Cano CE, Grasso D et al (2012) Nupr1-aurora kinase A pathway provides protection against metabolic stress-mediated autophagic-associated cell death. *Clin Cancer Res Off J Am Assoc Cancer Res* 18:5234–5246. doi:10.1158/1078-0432.CCR-12-0026
- Goruppi S, Iovanna JL (2010) Stress-inducible protein p8 is involved in several physiological and pathological processes. *J Biol Chem* 285:1577–1581. doi:10.1074/jbc.R109.080887
- Jiang WG, Davies G, Martin TA et al (2006) Com-1/p8 acts as a putative tumour suppressor in prostate cancer. *Int J Mol Med* 18:981–986
- Du P, Ye L, Yang Y, Jiang WG (2013) Candidate of metastasis 1 regulates in vitro growth and invasion of bladder cancer cells. *Int J Oncol* 42:1249–1256. doi:10.3892/ijo.2013.1802

28. Aumailley M, Battaglia C, Mayer U et al (1993) Nidogen mediates the formation of ternary complexes of basement membrane components. *Kidney Int* 43:7–12
29. Hopf M, Göhring W, Kohfeldt E et al (1999) Recombinant domain IV of perlecan binds to nidogens, laminin-nidogen complex, fibronectin, fibulin-2 and heparin. *Eur J Biochem FEBS* 259:917–925
30. Joyce JA, Pollard JW (2009) Microenvironmental regulation of metastasis. *Nat Rev Cancer* 9:239–252. doi:[10.1038/nrc2618](https://doi.org/10.1038/nrc2618)
31. Vasseur S, Hoffmeister A, Garcia-Montero A et al (2002) p8-deficient fibroblasts grow more rapidly and are more resistant to adriamycin-induced apoptosis. *Oncogene* 21:1685–1694. doi:[10.1038/sj.onc.1205222](https://doi.org/10.1038/sj.onc.1205222)